Dynamic behavior of quadrupolar orientational glasses: $K_xNa_{1-x}CN$ mixed crystals

Z. Hu, A. Wells, and C. W. Garland
Department of Chemistry and Center for Materials Science and Engineering, Massachusetts Institute of Technology, Cambridge, Massachusetts 02139
(Received 14 March 1991)

The ultrasonic velocity and attenuation of TA[100] acoustic waves have been measured as a function of temperature and frequency in $K_xNa_{1-x}CN$ mixed single crystals. Relaxation behavior is revealed by comparing our ultrasonic c_{44} elastic stiffness data with hypersonic c_{44} data obtained from Brillouin scattering. Combining ultrasonic velocity and attenuation data we are able to determine the Kramers-Kronig ratio R in the disordered paraelastic phase and to estimate it in the orientational glass phase. For the regime $\omega\tau_s \ll 1$, R is a direct measure of the cooperative quadrupolar clamped relaxation time τ_s, which can be represented by the empirical form $\ln\tau_s = A_s - B_sT$ in the paraelastic phase. Quadrupolar relaxation processes in the orientational glass state are also discussed.

I. INTRODUCTION

Mixed crystals of $K_xNa_{1-x}CN$ have attracted considerable recent interest because they exhibit an orientational glass phase.[1-8] In the dilute regimes $0 \le x < 0.15$ and $0.87 < x \le 1$, such mixed crystals undergo a weakly first-order soft-mode phase transition to a long-range orientationally ordered ferroelastic phase. In the broad intermediate composition range $0.15 < x < 0.87$, long-range order is frustrated and an orientational quadrupolar glass is observed at low temperatures.[1] Because there is no dilution of the pseudospin CN^- ions, no percolation effects occur. However, the random distribution of cations of different sizes has two effects—the lattice-mediated CN^--CN^- coupling is perturbed in the same way as in $K_xRb_{1-x}CN$ (where ordering occurs for all x),[8,9] and large quenched random-strain fields frustrate long-range quadrupolar (elastic) order.[10,11]

The phase diagram for $K_xNa_{1-x}CN$ mixed crystals was first established by dielectric and optical measurements[1,2] and has been confirmed by x-ray and neutron diffraction work.[3,4] This diagram is shown in Fig. 1, which also includes features obtained from our ultrasonic investigation. A detailed dielectric study on glassy $K_xNa_{1-x}CN$ crystals has revealed that *dipole* freezing follows an Arrhenius law with a broad distribution of dipolar relaxation times.[3] The *quadrupolar* freezing process has been characterized by studying the temperature dependence of the c_{44} elastic shear stiffness constant with inelastic neutron scattering,[3] Brillouin scattering,[7] ultrasonic measurements,[8] and shear-torque experiments.[5] The high-temperature static behavior of $c_{44}(T)$ in K-rich mixed crystals can be reasonably well described by Michel's random-strain-field model, but Na-rich mixed crystals show significant deviations from expectations based on this model.[8] Recently, Michel has extended his theory to include a nonergodic instability at the onset of the orientational glass phase.[12] This extended model has been used to explain the central peak intensity of quasielastic neutron scattering in a sample with $x = 0.89$.[6] It should be noted that there are many analogies between the $K_xNa_{1-x}CN$ quadrupolar glass system and $Rb_{1-x}(NH_4)_xH_2PO_4$ (RADP) dipolar glasses.[13]

In the present paper, we report the dynamic behavior of $K_xNa_{1-x}CN$ mixed crystals as determined with ultrasonic techniques. The elastic constant c_{44} associated

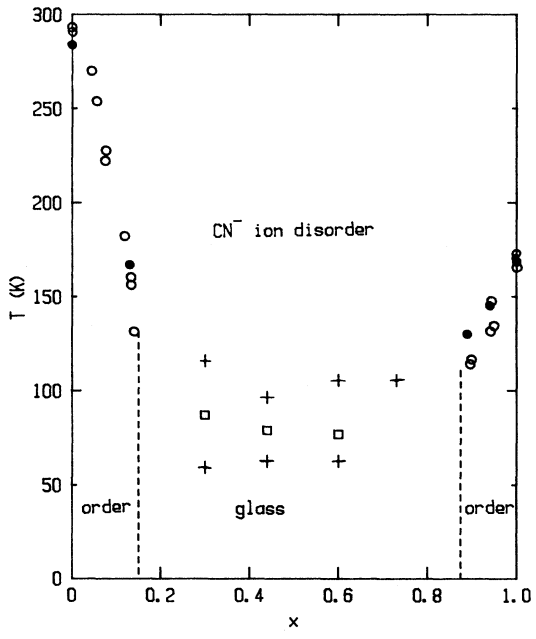

FIG. 1. Phase diagram for $K_xNa_{1-x}CN$ mixed single crystals. The order-disorder transitions for $x < 0.15$ and $0.87 < x$ are weakly first order, and transition temperatures $T_1(x)$ are based on dielectric data (○) from Ref. 1 and ultrasonic data (●) from Ref. 8. For samples forming an orientational glass, the ultrasonic echo pattern was lost on cooling and subsequently reestablished at a lower temperature, as marked by + symbols. The open squares indicate estimated values of the glass formation temperature T_g.

with the TA[100] acoustic mode involves a shear strain ϵ_4 with the same symmetry (T_{2g}) as the cyanide quadrupolar orientational order parameter Y. The velocity and attenuation of this TA[100] mode have been measured simultaneously as a function of temperature over the range 7–300 K. The results for $K_xNa_{1-x}CN$ are similar to but more detailed than those reported for the dynamics of $Rb(CN)_xBr_{1-x}$ mixed crystals.[14] In particular, ultrasonic data are now available in the orientational glass phase.

II. THEORY

The Michel quenched random strain model[10,11] for the *static* shear elasticity of cyanide crystals yields

$$\frac{c_{44}^b}{c_{44}(0)}=1+b\chi \ , \tag{1}$$

where $c_{44}(0)$ is the low-frequency limit of the TA[100] elastic constant, c_{44}^b is the "bare" stiffness expected in the absence of the $\gamma\epsilon_4 Y$ bilinear coupling term, χ is the dimensionless free (constant-stress) orientational order parameter susceptibility, and $b\equiv\gamma^2/c^b$ is a constant.[10,15] The susceptibility in the presence of random strain fields is given by $C(1-q)/[T-T_c(1-q)]$, where C is the Curie constant, T_c is the critical temperature at zero stress in the absence of random strains, and q is the Edwards-Anderson glass order parameter with the high-temperature form Σ/T^2. Thus one obtains

$$\frac{c_{44}^b}{c_{44}(0)}=\frac{T-T_c(1-q)}{T-T_0(1-q)} \ , \tag{2}$$

which provides a good description of $c_{44}(0)$ data for $Rb(CN)_xBr_{1-x}$, $K_xRb_{1-x}CN$, and $K_xNa_{1-x}CN$ in the disordered high-temperature phase.[8–10] It should, however, be stressed that in the case of $K_xNa_{1-x}CN$ the fitting parameters are physically reasonable for K-rich mixed crystals but artificial for Na-rich mixed crystals.[8]

In general, one needs to consider a complex frequency-dependent stiffness

$$c_{44}(\omega)=c_{44}^b+\Delta c_{44}(\omega) \ , \tag{3}$$

where $\Delta c_{44}(\omega)=\Delta c'_{44}(\omega)+i\Delta c''_{44}(\omega)$ is the (negative) complex "critical" or "configurational" contribution. This quantity is given by

$$-\Delta c_{44}(\omega)=\gamma^2\chi_{\rm cl}(\omega) \ , \tag{4}$$

where γ is the bilinear coupling constant and $\chi_{\rm cl}(\omega)$ is the clamped (constant-strain) susceptibility ($\chi_{\rm cl}^{-1}=\chi^{-1}+\gamma^2/c^b$). It follows that

$$-\Delta c'(\omega)=\gamma^2\chi'_{\rm cl}(\omega)=c_\infty-c \ , \tag{5a}$$

$$-\Delta c''(\omega)=\gamma^2\chi''_{\rm cl}(\omega)=2\rho v^3\Delta\alpha/\omega \ , \tag{5b}$$

$$R\equiv\frac{1}{\omega}\frac{\chi''_{\rm cl}}{\chi'_{\rm cl}}=\frac{1}{\omega}\frac{\Delta c''}{\Delta c'}=\frac{c}{(c_\infty-c)}\frac{2v\Delta\alpha}{\omega^2} \ , \tag{5c}$$

where R is the Kramers-Kronig ratio. The subscript 44 has been dropped, and c_∞ is the infinite-frequency limit ($=c^b$ from the above formulation). The quantity $c\equiv c(\omega)=\rho v^2$ is the real part of the complex stiffness, where ρ is the mass density and v is the TA[100] shear velocity at frequency $\omega=2\pi f$. The quantity $\Delta\alpha$ is the cooperative configurational attenuation at ω.

For a simple Debye relaxation, one obtains the familiar elastic relaxation equations[16] and $R=\tau_s=(c_0/c_\infty)\tau$, where c_0 is the static stiffness, τ_s is the constant-strain relaxation time, and τ is the free (constant-stress) relaxation time. In the case of critical behavior associated with long-range ordering, linear response theory and dynamic scaling concepts yield more general expressions for $-\Delta c'(\omega)$, $-\Delta c''(\omega)$, and R:[17]

$$-\Delta c'(\omega)=C(T)G(\omega\tau) \ , \tag{6a}$$

$$-\Delta c''(\omega)=\left[\frac{\mu}{z\nu}\right]C(T)\omega\tau F(\omega\tau) \ , \tag{6b}$$

$$R=\left[\frac{\mu}{z\nu}\right]\tau\frac{F(\omega\tau)}{G(\omega\tau)}\cong\left[\frac{\mu}{z\nu}\right]\frac{\arctan\omega\tau}{\omega} \ , \tag{6c}$$

where the relaxation strength $C(T)$ varies like $(T-T_c)^{-\mu}$ and the free relaxation time τ varies like $(T-T_c)^{-z\nu}$ near a fluctuation-dominated critical point. The scaling functions $F(\omega\tau)$ and $G(\omega\tau)$ both equal unity in the $\omega\tau\ll1$ limit; their complete forms are given in Ref. 17. The approximate form for R given in Eq. (6c) is a good approximation for all $\omega\tau$ when $\mu/z\nu\le0.25$. In this case, the Kramers-Kronig ratio has the limits $R\to(\mu/z\nu)\tau$ for $\omega\tau<0.2$ and $R\to(\mu/z\nu)(\pi/2\omega)$ for $\omega\tau>30$. In the limiting case where $\mu/z\nu=1$, $R=\tau$ for all $\omega\tau$. For cyanide mixed crystals that exhibit long-range orientational orderings, Eqs. (6) should pertain with some modified version of the τ temperature dependence. "Smeared" or rounded versions of such critical behavior might be observed due to the influence of nonzero random strain fields.

For cyanide mixed crystals that form an orientational glass phase at low temperature, it seems more appropriate to utilize a temperature-dependent distribution of relaxation processes $g(\tau,T)$ that becomes very broad at low temperatures. In view of the analogy between quadrupolar cyanide glasses and the RADP dipolar glasses, we have followed the treatment of Courtens *et al.*[13] in assuming a rectangular (flat) distribution of constant-strain relaxation times with a short-time cutoff τ_m and a long-time cutoff τ_c. The latter value is strongly temperature dependent. For this model, one has

$$\chi_{\rm cl}(\omega,T)=\chi^0_{\rm cl}(T)I(\omega\tau)=\chi^0_{\rm cl}(T)\int_0^\infty\frac{g(\tau,T)}{1-i\omega\tau}d\ln\tau \ , \tag{7}$$

where $\chi^0_{\rm cl}(T)$ is the clamped static susceptibility,[13] and

$$R=\frac{1}{\omega}\frac{\arctan(\omega\tau_c)-\arctan(\omega\tau_m)}{\ln(\tau_c/\tau_m)-\frac{1}{2}\ln[(1+\omega^2\tau_c^2)/(1+\omega^2\tau_m^2)]} \ . \tag{8}$$

This expression for the Kramers-Kronig ratio has several limiting regimes of interest:

$$\text{(i)}\quad R=\frac{\tau_c}{\ln(\tau_c/\tau_m)}, \quad \text{for } \omega\tau_m\ll1, \ \ \omega\tau_c\le0.4 \ , \tag{9}$$

(ii) $$R=\frac{1}{(-\ln\omega\tau_m)}\frac{\arctan\omega\tau_c}{\omega},$$

$$\text{for } \omega\tau_m \ll 1, \quad \omega\tau_c > 10, \tag{10a}$$

$$\rightarrow \frac{1}{(-\ln\omega\tau_m)}\frac{\pi}{2\omega},$$

$$\text{for } \omega\tau_m \ll 1, \quad \omega\tau_c > 30, \tag{10b}$$

and

$$\text{(iii)} \quad R \cong 2\tau_m, \quad \text{for } \omega\tau_m \geq 10, \quad \omega\tau_c \rightarrow \infty . \tag{11}$$

The available cyanide data in the disordered paraelastic phase fall in the $\omega\tau$ regime of Eq. (9) and low-temperature data deep in the glass phase should conform to Eq. (10). It appears that the regime of Eq. (11) is never realized for ultrasonic data on cyanide mixed crystals.

III. EXPERIMENTAL RESULTS

The $K_xNa_{1-x}CN$ single crystals have been described previously in connection with a study of the temperature dependence of the static acoustic velocity in the paraelastic regime.[8] For the present investigation, the surfaces of the samples were further polished to reduce any nonparallelity to less than 1 μm in a thickness of $\sim$5 mm. The room-temperature lattice parameters determined by powder x-ray diffraction were well described by the linear relationship $a(\text{Å})=5.886+0.635x$, which agrees well with recent neutron diffraction measurements.[3,4]

The ultrasonic measurements were made with a coherent phase-sensitive technique that has a wide dynamic range and good single-to-noise ratios for weak signals. See Ref. 10 for details of the method and acoustic bonding of the lithium niobate transducer to the sample. The only modification of the previous procedure was to use propyl and isobutyl alcohol as bonding materials in the 80 K $< T <$ 170 K range.

The velocity v and attenuation α of shear waves propagating in the [100] direction were measured simultaneously as a function of temperature for several frequencies ($\sim$10, 32, 54 MHz) in five $K_xNa_{1-x}CN$ samples with $x=0.30$, 0.44, 0.60, 0.73, and 0.88. Temperature was scanned slowly (less than 2 K/h in critical regions), and the agreement between cooling and warming runs was good. No velocity dispersion (i.e., no frequency dependence of v) was observed; 10-MHz-velocity data are presented since reliable absolute values are available over the most extensive temperature range.

The temperature dependence of the elastic stiffness $c_{44}=\rho v^2$ and the 10-MHz attenuation α are shown for samples with $x=0.30$, 0.44, and 0.60 in Figs. 2, 3, and 4, respectively. In each case there is a region where data are missing due to a very high level of attenuation. On cooling, the echo pattern became progressively weaker until all the echoes disappeared. Then after further cooling, echoes slowly reappeared at a lower temperature. This change in echo pattern was reversible on heating, and "annealing" the sample for $\sim$4 h in the gap did not cause any echo pattern to develop. A similar behavior was observed for a $Rb(CN)_xBr_{1-x}$ sample with

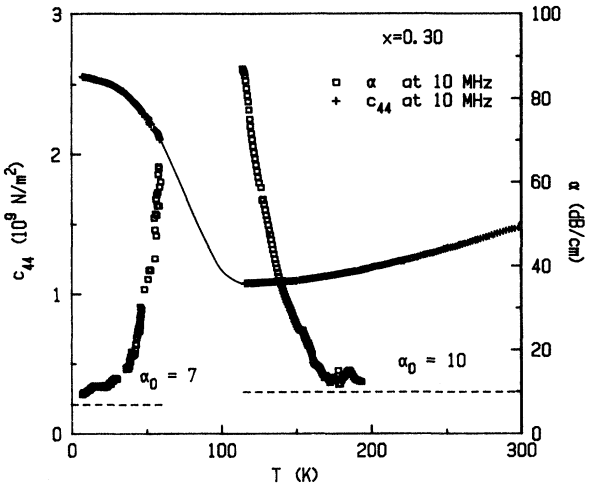

FIG. 2. Shear stiffness c_{44} and acoustic attenuation α for $K_{0.30}Na_{0.70}CN$. The smooth curve is an estimate of c_{44} in the gap.

$x=0.19$.[10] The background attenuation level α_0 shown in Figs. 2–4 represents the noncritical contribution observed far from the phase transition or glass formation temperature. The value of α_0 is independent of T in the paraelastic phase (over the 90–170 K range)[14] and in the glass phase.

The c_{44} data in the paraelastic phase (90–300 K) have been analyzed previously[8] in terms of a quenched-random-strain-model. Using the fitting parameters obtained for this model, one can calculate T_f, defined as the temperature where c_{44} should go through a minimum value for glass-forming samples or go to zero for samples that exhibit long-range order.[10] The glass-formation tem-

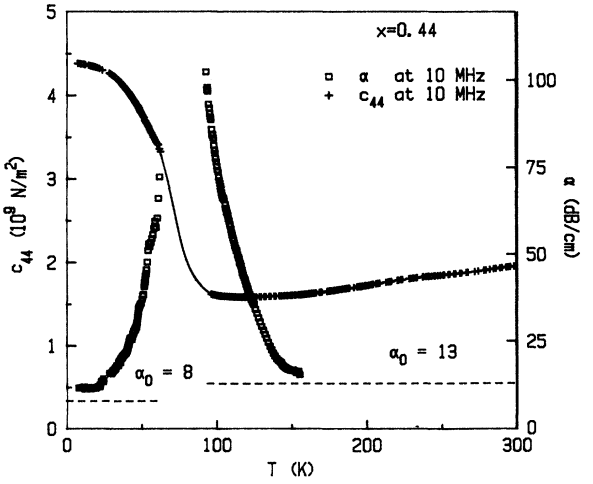

FIG. 3. Shear stiffness c_{44} and attenuation α for $K_{0.44}Na_{0.56}CN$. The smooth curve is an estimate of c_{44} in the gap.

perature T_g lies below T_f and estimates of T_g defined as the attenuation maximum at 10 MHz are given in Fig. 1.

Attenuation data were also obtained on two other samples, but only in the paraelastic phase. For a sample with $x=0.73$, the echo pattern below T_g was too weak and distorted to provide reliable data. For a sample with $x=0.88$, long-range ordering occurs at ~ 130 K and scattering from antiphase domains destroys the echo pattern, as it does for $K_xRb_{1-x}CN$ crystals.[9] The paraelastic attenuation in these two samples is shown together with that from the other samples in Fig. 5. This figure presents the temperature dependence of $\Delta\alpha/\omega^2$ calculated from 10-MHz data. All ultrasonic attenuation data in the paraelastic phase of $Rb(CN)_xBr_{1-x}$ vary like ω^2; this quadratic scaling is likely but has not been established for $K_xNa_{1-x}CN$. Due to pulse distortion and high attenuation levels, no reliable α data could be obtained in the paraelastic phase at 32 and 54 MHz. The best high-frequency data were obtained at 30 MHz for the $x=30$ and 0.44 samples over the range 100–120 K. These data could not be scaled quadratically onto the 10 MHz $\Delta\alpha(T)$ curve, but the poor echo pattern (a single distorted echo) and very limited frequency and temperature range make this observation inconclusive.

Only 10-MHz data could be obtained below T_g for the samples with $x=0.30$ and 0.44. In the case of $K_{0.6}Na_{0.4}CN$, low-temperature data were obtained at three frequencies in the glass phase and the attenuation variations are shown in Fig. 6. The 10-MHz attenuations are accurate absolute values based on two echoes. However, the 32- and 54-MHz attenuations are relative values based on the temperature dependence of the magnitude of the first echo (the only undistorted echo observable). Their absolute values can be roughly estimated from previous experience with echo patterns on the oscilloscope but not precisely established. We have proceeded by assuming that $\Delta\alpha=\alpha-\alpha_0$ should scale with frequency like

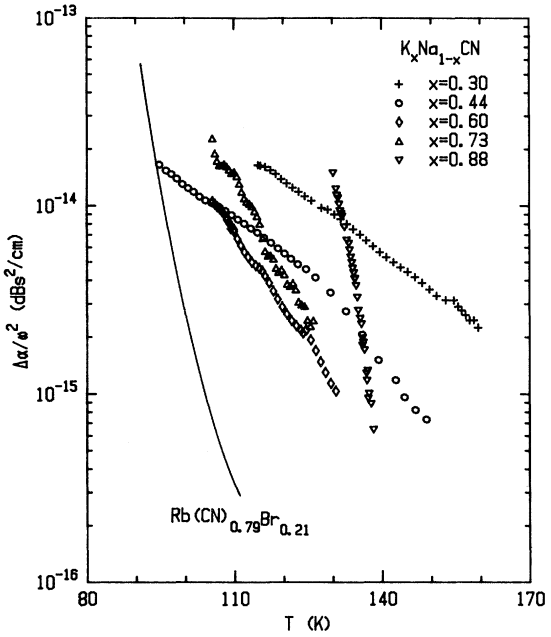

FIG. 5. Semilog plot of $\Delta\alpha/\omega^2$ vs T for 10-MHz data in the disordered paraelastic phase. The sample with $x=0.88$ undergoes a phase transition into an ordered phase at $T_1\simeq 130$ K. The smooth curve for the rubidium mixed crystal is taken from Ref. 14.

ω^n. With the values α(32.4 MHz) and α(54.4 MHz) shown in Fig. 6, one obtains an excellent scaling over a range of ~ 20 K with $n=1.3$, as shown in Fig. 7. Indeed, the limits on n are rather tight: $n=1.3\pm 0.15$ for 95% confidence limits. A ω^2 frequency dependence for $\Delta\alpha$ in the range $T<50$ K cannot be achieved with any shift in α(32 MHz) or α(54 MHz) values; thus the present data are inconsistent with ω^2 scaling. The solid line in Fig. 7 is the best fit with an empirical form $\Delta\alpha/\omega^{1.3}=(1.77\times 10^{-10})\exp(0.064T)$.

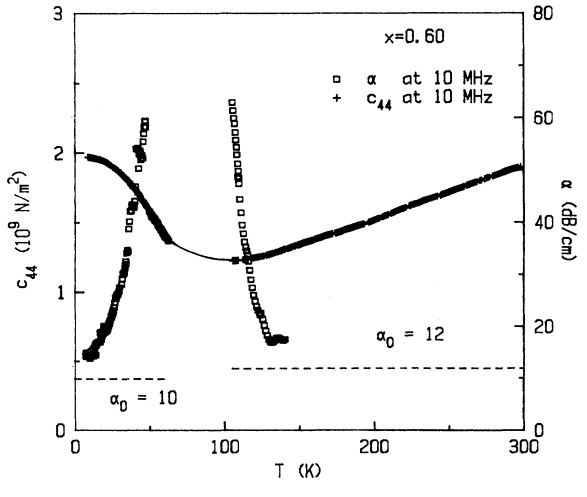

FIG. 4. Shear stiffness c_{44} and attenuation α for $K_{0.60}Na_{0.40}CN$. The smooth curve is an estimate of c_{44} in the gap.

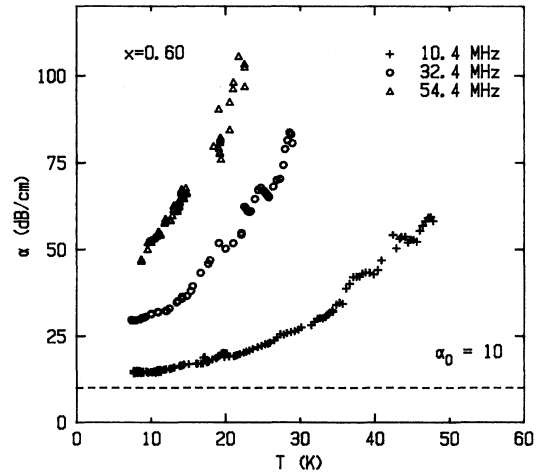

FIG. 6. Temperature dependence of acoustic attenuation for $K_{0.60}Na_{0.40}CN$ at three frequencies in the glass phase.

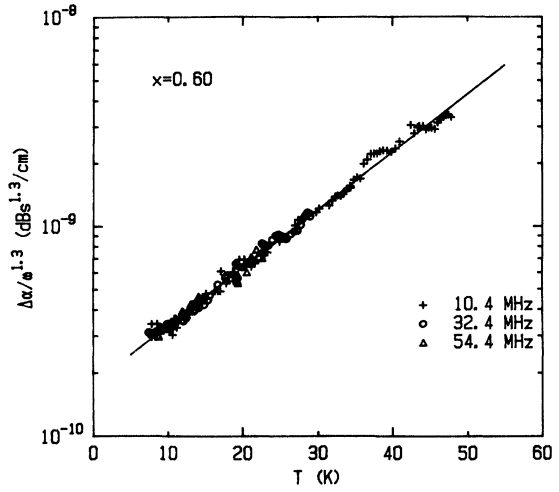

FIG. 7. Scaling plot of $K_{0.60}Na_{0.40}CN$ attenuation data in the glass phase (see text).

IV. DATA ANALYSIS AND DISCUSSION

A previous analysis[8] of the static elastic shear behavior for temperatures above T_g has shown that K-rich mixed crystals were quite well described by an extended version of the quenched-random-strain model but that Na-rich crystals exhibit significant systematic deviations from the model. We are concerned here with the dynamic aspects

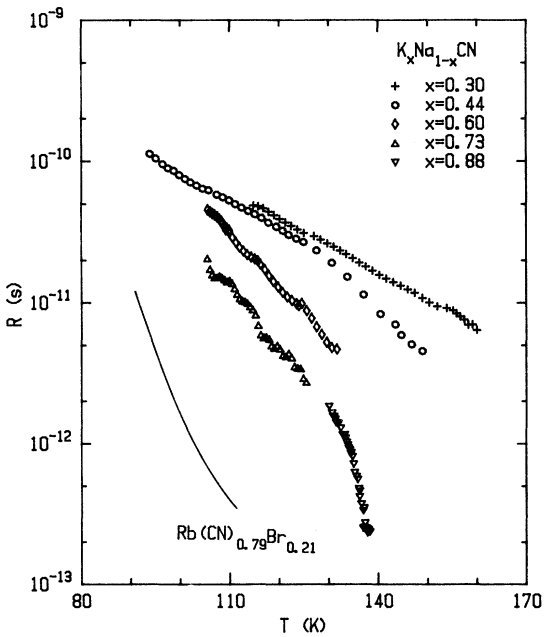

FIG. 8. Kramers-Kronig ratio R given by Eq. (5c) for $K_xNa_{1-x}CN$ samples. The line indicates the R values of $Rb(CN)_{0.79}Br_{0.21}$ taken from Ref. 14. For $\omega\tau_s \ll 1$ as here, R is a direct measure of the cooperative constant-strain relaxation time τ_s.

of shear elasticity in the paraelastic regime and with the behavior of c_{44} and $\Delta\alpha$ in the orientational glass phase.

Let us first consider the sample with $x=0.88$, which is the only one investigated that undergoes a phase transition into a long-range ordered phase. As shown in Fig. 5, the temperature dependence of the attenuation for this sample is considerably different from the other $K_xNa_{1-x}CN$ crystals but closely resembles that for $Rb(CN)_{0.79}Br_{0.21}$, which also undergoes a phase transition.[10,14] Taking $\tau=(c_\infty/c_0)R$, using $c_0=c(10\text{ MHz})$ and $c_\infty=c^{\text{bare}}=5.68\times10^9$ N/m^2 (value given in Ref. 8), and representing τ by

$$\tau=\tau_0|(T-T_f)/T_f|^{-z\nu}\equiv\tau_0|t|^{-z\nu} \tag{12}$$

as was done for $Rb(CN)_{0.79}Br_{0.21}$, we find from a least-squares fit $\tau_0=2.36\times10^{-15}$ s and $z\nu=4.5$. The T_f value was held fixed at 119 K, which is the value obtained from the static velocity fit. This power-law variation of τ for $K_{0.88}Na_{0.12}CN$ must be viewed with considerable caution since (a) only a very narrow t range is available (0.09–0.18), (b) there was a distortion of the echo shape when T was close to T_f and (c) any concentration gradients would play a large role because $x=0.88$ is just at the boundary x_c between regimes of long-range order and orientational glass formation (see Fig. 1). The critical exponent $z\nu=4.5$ is far from the conventional van Hove value ($z\nu=1$) that is found for KDP-type ferroelectrics having bilinear piezoelectric coupling[16] and from critical fluctuation values ranging from $z\nu=1.28$ (3D Ising) to $z\nu=1.43$ (3D Heisenberg).[18] It is, however, quite similar to the value $z\nu=3.7$ obtained for $Rb(CN)_{0.79}Br_{0.21}$.[14] Furthermore, there are theoretical predictions that $z=6$ for a spin glass,[19] in which case $z\nu=3$ to 4 since $\nu=\frac{1}{2}$ (mean-field) to $\sim\frac{2}{3}$ (critical fluctuation). Perhaps these random-strain cyanide systems are more closely related to spin glasses than critical order-disorder systems.

Returning to Fig. 5, it is clear that for samples forming orientational glasses the behavior of $\Delta\alpha$ above T_g is different for K-rich ($x=0.60$ and 0.73) and Na-rich ($x=0.44$ and 0.30) samples. The Kramers-Kronig ratios R as calculated from Eq. (5c) are shown in Fig. 8 in the paraelastic regime for $x=0.30$, 0.44, 0.60, 0.73, and 0.88 samples. A smooth curve representing the data for $Rb(CN)_{0.79}Br_{0.21}$ (Ref. 14) is also included for comparison. These R values were calculated with the assumption that c_∞ values are equal to the c^b values given in Ref. 8. For $\omega\tau_s \ll 1$, R is a direct measure of the cooperative constant-strain relaxation time τ_s. Upon cooling, the quadrupolar relaxation time increases as expected since the system is freezing into an orientational glass state.

The R (or τ_s) values for $T>T_g$ in glassy $K_xNa_{1-x}CN$ samples ($0.15<x<0.87$) can be well represented by the empirical expression

$$\ln\tau_s\simeq\ln R=A_s-B_sT\ , \tag{13}$$

which is also observed for $Rb(CN)_xBr_{1-x}$ samples with $x<x_c$. Values of parameters A_s and B_s are given in Table I, along with the analogous A and B that represent

TABLE I. Least-squares values of the parameters A_s and B_s in $\ln\tau_s = A_s - B_s T$ and A and B in $\ln\tau = A - BT$, where τ_s and τ are the relaxation times at constant strain and constant stress respectively. The temperature range of each fit is also given.

x	T range (K)	A_s	B_s	χ_ν^2	A	B	χ_ν^2
0.30	115–160	−18.58	0.045	0.98	−16.56	0.045	0.99
0.44	94–132	−18.77	0.045	0.93	−17.31	0.044	1.05
	132–150	−14.31	0.080	1.01	−12.61	0.080	1.01
0.60	106–132	−14.48	0.088	1.16	−12.57	0.090	1.19
0.73	106–126	−14.39	0.097	1.62	−10.78	0.106	1.68
0.88	130–139	9.93	0.282	5.41	21.81	0.344	4.10

the $\ln\tau = A - BT$ behavior, where τ is the relaxation time at constant stress. The R values for the $x = 0.88$ sample exhibit systematic deviations from Eq. (13) at the low-temperature end of its narrow range, which distinguish this sample from glassy samples. Note also that the R curve for the $x = 0.44$ sample bends rather sharply at ~132 K. Parameters for $x = 0.44$ were obtained by fitting Eq. (13) to data over two temperature ranges: 94–132 K and 132–150 K.

We have also tried other functional forms for τ that are commonly used to describe the relaxation behavior in glassy systems[20], including an Arrhenius law $\tau = \tau_\infty \exp(E/T)$, a Vogel-Fulcher law $\tau = \tau_\infty \exp[E/(T - T_0)]$, and a power law. None of these yields satisfactory results, in agreement with the conclusions of our analysis of the quadrupolar acoustic relaxation in glassy $Rb(CN)_xBr_{1-x}$ samples.[14] In spite of the systematic character of the deviations, the poor χ_ν^2 values, and physically unreasonable parameter values (see Ref. 14), Arrhenius fitting parameters are given in Table II to facilitate a comparison with published fits to dipolar relaxation behavior as determined from dielectric measurements on $K_xNa_{1-x}CN$.[3] There is no real correspondence between these two relaxation probes: dielectric data characterize the single CN^- electric dipole reorientation and ultrasonic data characterize the cooperative quadrupolar relaxation. Dipolar relaxation is 10 to 50 times more rapid than quadrupolar, and its temperature dependence is different.[3] Although the phase diagram for $K_xNa_{1-x}CN$ strongly resembles that for the dipolar glass systems RADP, the dynamic behavior seems different. For the latter system, the cooperative (dipolar) relaxation time follows a Vogel-Fulcher law over a wide temperature range.[13] For the cyanide system, τ grows *more slowly* on cooling than expected from an Arrhenius fit rather than more rapidly as required for a Vogel-Fulcher form. That is, deviations from Arrhenius behavior are *opposite* to those modelled by the Vogel-Fulcher form, as was also observed for $Rb(CN)_xBr_{1-x}$.[14] Unfortunately, these ultrasonic data characterize τ only over a narrow range of ~40 K.

Not enough data are available to allow a more extensive analysis of the $x = 0.73$ sample, but low-temperature ($T < T_g$) data exist for the other three glass formers and they will be analyzed over the temperature range 0–150 K along with analogous data for $Rb(CN)_{0.19}Br_{0.81}$ over the 0–55 K range (see Fig. 3 in Ref. 10). In addition to ultrasonic c_{44} and $\Delta\alpha$ data in the orientational glass phase for samples with $x = 0.30$, 0.44, and 0.60, there are recent Brillouin scattering c_{44} data over the entire 0–300 K range for $K_xNa_{1-x}CN$ crystals with $x = 0.19$, 0.31, and 0.59.[7] This allows a direct characterization of dispersion effects for the latter two samples. The elastic constants c_{44} measured by ultrasonic (US) techniques at 10 MHz and Brillouin scattering (BS) techniques at ~6 GHz are shown as a function of temperature in Figs. 9 and 10 for the $x = 0.30$ and 0.60 samples, respectively. The smooth curves are alternate choices for the infinite frequency limit c_∞, which will be discussed later.

Inspection of Figs. 9 and 10 shows a clear velocity dispersion at intermediate temperatures near T_g but rather little dispersion at the lowest temperatures or above ~170 K. In the paraelastic regime far above T_g (say $T > T_g + 75$ K), there is no dispersion between BS and US data for $x = 0.60$ and only a small "non-critical" (temperature-independent) dispersion for $x = 0.30$. The

TABLE II. Least-squares values of the parameters E and τ_∞ in the Arrhenius expression $\tau = \tau_\infty \exp(E/T)$. It should be stressed that this form provides a poor representation of the data (see text).

x	T range (K)	$E(K)$	τ_∞ (s)	χ_ν^2
0.30	115–160	825	3.19×10^{-13}	5.70
0.44	94–132	552	1.56×10^{-12}	4.86
0.60	106–132	1231	2.44×10^{-15}	2.29
0.73	106–126	1398	5.30×10^{-16}	2.05
0.88	130–139	3486	2.22×10^{-22}	5.03

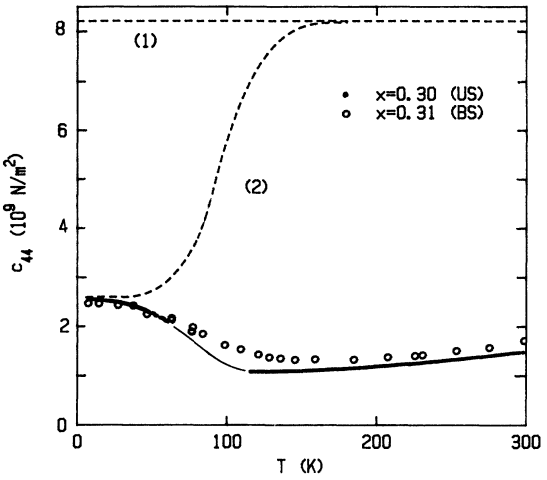

FIG. 9. Ultrasonic (US) shear stiffness data at 10 MHz and Brillouin scattering (BS, Ref. 7) data at ~6 GHz for $K_{0.3}Na_{0.7}CN$, together with two choices of c_∞: (1) $c_\infty = c^{\text{bare}}$ for all temperatures, (2) $c_\infty = c^{\text{bare}}$ for $T > 180$ K and a lower c_∞ choice for $T < 180$ K (see text).

presently available data are not conclusive, but it appears that no dispersion occurs in the high-temperature paraelastic regime for K-rich samples, but a small temperature-independent dispersion does occur for Na-rich samples. Behavior similar to that exhibited in Fig. 9 can be inferred for a $x = 0.19$ sample, where both Brillouin and neutron scattering (NS) data are available.[6,7]

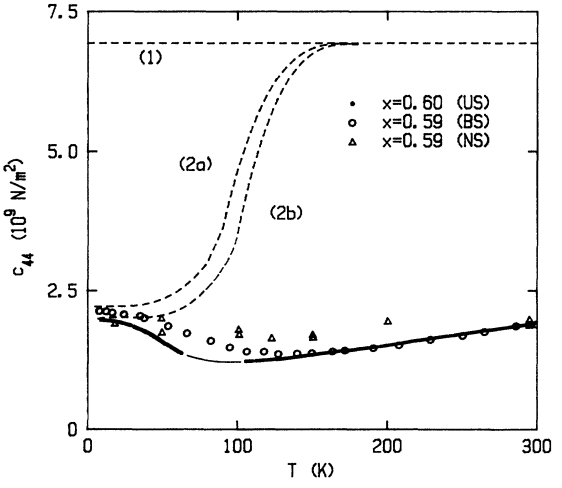

FIG. 10. Ultrasonic (US) shear stiffness data at 10 MHz, Brillouin scattering (BS, Ref. 7) at ~6 GHz, and neutron scattering (NS, Ref. 6) data at ~0.7 THz for $K_{0.6}Na_{0.4}CN$, together with three choices of c_∞: (1) $c_\infty = c^{\text{bare}}$ for all temperatures, (2a) and (2b) $c_\infty = c^{\text{bare}}$ for $T > 160$ K and lower c_∞ choices for $T < 160$ K (see text). The absolute values of the NS data are somewhat unreliable, and NS data points have been shifted up by 0.7×10^9 N/m^2 to avoid unphysical negative dispersion at low temperature and near room temperature.

The BS and NS data agree well for $T > 200$ K and $T < 60$ K and show dispersion at intermediate temperatures. By interpolating between our published ultrasonic data for $x = 0.13$ and 0.30,[8] we can obtain an estimate of c_{44} at 10 MHz for $x = 0.19$. This US c_{44}-vs-T curve is parallel to but 0.3×10^9 N m^{-2} below the BS curve over the range 165–300 K. Between ~130 K and 165 K the US curve lies even lower, as expected in the region of "critical" dispersion on approaching T_g. A temperature-independent dispersion between BS and US elastic constants has also been observed in pure NaCN, where the effect has been attributed either to noncritical dispersion or to the existence of inhomogeneous structures in the crystal.[21] Specifically, inhomogeneities due to mosaic grains are quite common for Czochralski-grown samples, and angular-resolved Brillouin scattering has revealed such mosaic regions in $Na(CN)_xCl_{1-x}$ mixed crystals.[21] In contrast to this, there is no high-temperature paraelastic BS/US dispersion in pure KCN or CN-rich mixed crystals of $K(CN)_xBr_{1-x}$ or $K(CN)_xCl_{1-x}$.[22]

The temperature-independent dispersion between US and BS c_{44} data in the paraelastic regime of Na-rich samples cannot be explained by experimental errors. Although the room-temperature density and path length are used for calculation of the ultrasonic elastic constant over the entire temperature range, the error due to this is estimated to be less than 1%. The approximation of using room-temperature density and refractive index only yields a 1% error in Brillouin elastic constant data.[7] The difference in the noncritical high-temperature dispersion behavior between Na-rich samples and K-rich samples is not surprising since previous studies have revealed significant differences between Na-rich and K-rich crystals: (a) different orientational probability functions for the cyanide ion in Na- and K-rich crystals are shown in a neutron diffraction experiment;[3] (b) the static shear elastic constants of K-rich samples are in better agreement with the random strain model than those of Na-rich samples;[8] (c) an x-ray study shows that samples with $x < 0.05$ exhibit a first-order phase transition with the lattice constant undergoing a 5% change, whereas samples with $x > 0.95$ undergo almost second-order phase transitions with only a 1% change in lattice constant.[23] The asymmetry in the behavior of Na-rich and K-rich crystals is also supported by a recent molecular dynamics calculation[24] which shows that there are two different local ordering mechanisms: Na^+ ions act as nucleation centers to align neighboring CN^- along a [100] direction, while K^+ ions tend to align neighboring CN^- along a [111] orientation.

In summary, critical (temperature-dependent) shear velocity dispersion between US and BS data is observed on cooling below $T_g + 75$ K and disappears again at low temperatures. For the available US data in the paraelastic regime above T_g, $\omega\tau_s \ll 1$ as in the disordered phase of most order-disorder systems.[25] In the glass phase at low temperatures, the absence of dispersion indicates that $\omega\tau_s \ll 1$ or $\omega\tau_s \gg 1$ for data over the 10–700 GHz range.

Let us now consider the analysis of cooperative dynamical behavior in the orientational glass phase. In order to extract τ values from the experimentally known

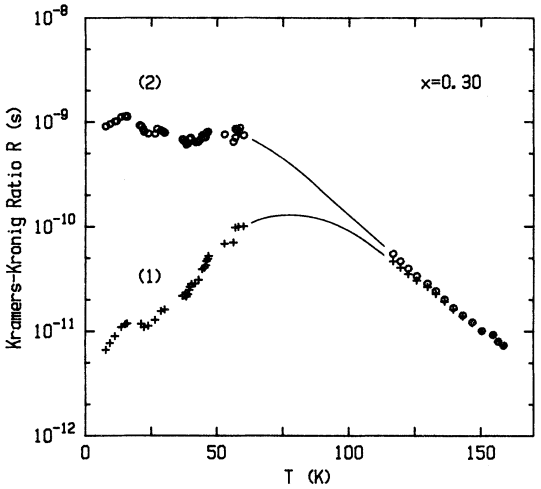

FIG. 11. Kramers-Kronig ratio R as a function of T for the $x=0.30$ sample as calculated from Eq. (5c). Curves (1) and (2) correspond to choices (1) and (2) for the c_∞ values shown in Fig. 9. The solid lines are guides for the eye.

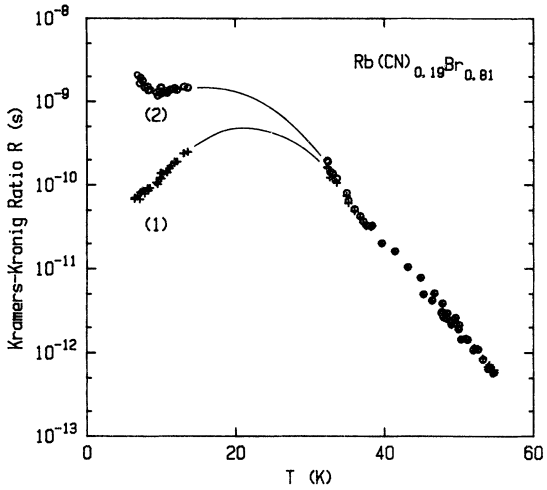

FIG. 13. Kramers-Kronig ratio R as a function of T for $Rb(CN)_{0.19}(Br)_{0.81}$. Experimental data taken from Refs. 10 and 14. Curve (1) is based on $c_\infty = c^{\text{bare}} = 3.95\times10^9$ N/m^2 as obtained in Ref. 10 from fits to the *static* elastic behavior. Curve (2) is based on $c_\infty = 2.20\times10^9$ N/m^2 for $T<15$ K rising smoothly to $c_\infty = c^{\text{bare}}$ for $T>35$ K, much like curve (2) in Fig. 9.

$-\Delta c''(\omega)$, one must determine the relaxation strength [$C(T)$ or $\gamma^2\chi^0_{\text{cl}}(T)$] and the form of the frequency-dependent relaxation function [$(\mu/z\nu)\omega\tau F(\omega\tau)$ or $I''(\omega\tau_s)$]. The relaxation strength equals $(c_\infty - c_0)$; thus its determination requires both c_∞ and c_0 (the $\omega\to0$ limiting stiffness) as functions of temperature. In the case of paraelastic data, the situation is simple: $c_0 = c(10\text{ MHz})$, c_∞ is known from independent *static* fits with the quenched random-strain-field model, and the relaxation function is simply $\omega\tau$. However, in the glass phase the situation is more complicated: c_0 is uncertain,[5] c_∞ is not known, and the relaxation function is complicated and imperfectly known. A better general approach for the evaluation of τ is to use the Kramers-Kronig ratio R. The determination of R requires only known c and $\Delta\alpha$ data plus a choice of $c_\infty(T)$. The interpretation of R requires only the ratio of the imaginary and real parts of the complex relaxation function [$(\mu/z\nu)\omega\tau F(\omega\tau)/G(\omega\tau)$ or $I''(\omega\tau_s)I'(\omega\tau_s)$], which has a simpler form than the imaginary part alone. This approach was already used in Fig. 8 for the determination of the τ_s behavior in the paraelastic phase.

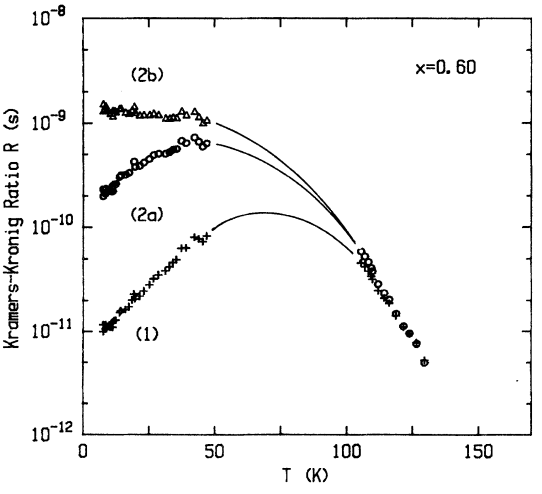

FIG. 12. Kramers-Kronig ratio R as a function of T for the $x=0.60$ sample as calculated from Eq. (5c). Curves (1), (2a), and (2b) correspond to the choices for c_∞ values shown in Fig. 10. The solid lines are guides for the eye.

The behavior of R over the 7–150 K temperature range for $K_xNa_{1-x}CN$ samples with $x=0.30$ and 0.60 is shown in Figs. 11 and 12, respectively. The R values for $x=0.44$, which are not shown, are very similar ($\sim10\%$ larger) to those for $x=0.30$. The analogous plot for $RbCN_{0.19}Br_{0.81}$ (for detailed data, see Ref. 10) is presented in Fig. 13 over the temperature range 7–60 K for comparison.

The R values in Figs. 11–13 are based on two limiting choices of $c_\infty(T)$: (1) a large T-independent value $c_\infty = c^b$ and (2) a low c_∞ value that is constant in the 0–30 K range and then rises to become c^b above ~160 K. These alternative c_∞ choices are shown in Figs. 9 and 10. The c^b values represent a linear interpolation between the bare c_{44} values for pure NaCN and KCN and are the same values that were used in our analysis of the static elastic behavior in the paraelastic phase.[8] The rationale for choice (2) c_∞ values is the fact that little or no dispersion is seen below ~60 K for c_{44} obtained with US, BS, or NS techniques, which suggests that $\omega\tau$ is very large as expected for a glass phase. Thus the low-temperature c_∞ value is chosen to be close to the observed c_{44} at 7 K, and c_∞ is joined smoothly to c^b in the

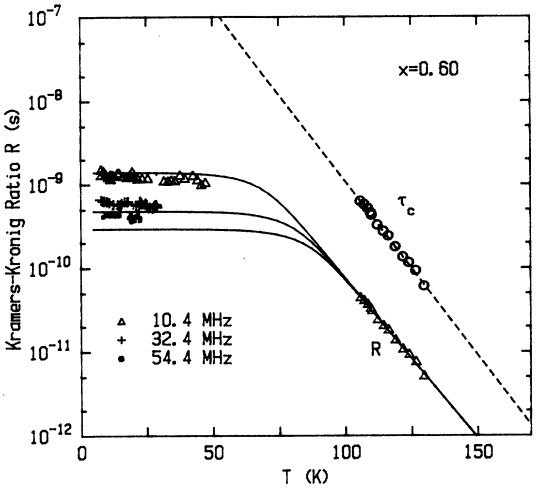

FIG. 14. Fit of R for $K_{0.6}Na_{0.4}CN$ with a broad rectangular distribution function $g(\tau,T)$ for which the short-time limit is $\tau_m = 5\times10^{-16}$ s and the temperature-dependent long-time cutoff time τ_c is given by the open circles and the dashed line.

dispersion-free paraelastic region. Recently, Michel has proposed that the quadrupolar order parameter susceptibility χ should include both a quenched-random-strain field contribution and a nonergodic contribution. The quantity χ_{ne} is zero above T_g, has a positive constant value for low T and small wave vectors, and varies rapidly over a narrow temperature range around T_g. A sharp decrease in c_∞ around T_g may be related to this nonergodic effect.

The low-temperature R values obtained with choice (1) for c_∞ represent lower limits and do not seem physically attractive. The overall pattern on cooling (increasing R in the paraelastic phase, a broad maximum near T_g, and a subsequent decrease) suggests a strongly smeared version of critical behavior near an order-disorder transition[17] rather than the expected monotonic increase in τ associated with glass formation. Furthermore, this choice implies $\omega\tau \ll 1$ deep in the glass phase, which would require $\Delta\alpha\sim\omega^2$ frequency dependence and c_{44} (US) $\cong c_{44}$(BS) equal to c_0. The former is inconsistent with our $\Delta\alpha\sim\omega^{1.3}$ scaling of $x=0.60$ glass phase data, and the latter is inconsistent with 0.1-Hz shear-torque measurements.[5] Furthermore, recent elastic field experiments[26] on cyanide quadrupolar glasses has revealed that the field-cooled behavior of a cyanide glass is essentially the same as the behavior of a spin glass. Specifically, the field-cooled strain decays in time following a Kohlrausch-Williams-Watts law which represents typical glass relaxation behavior. This further demonstrates that the quadrupolar freezing process is not a smeared version of order-disorder critical behavior.

The low-temperature R values obtained with c_∞ choice (2) for the $x=0.30$ sample and choice (2b) for the $x=0.60$ sample are much more reasonable. An orientational glass characterized by a monotonic increase in τ on cooling and a very broad temperature-dependent relaxation function can be described with Eqs. (8)–(11). At high-temperatures, where $\omega\tau_m \ll \omega\tau_c < 1$, R should conform to Eq. (9). Thus the increase in R on cooling is due to the rapid increase in τ_c. The flat plateau in R at low temperatures is expected from Eqs. (10a) and (10b) if $\omega\tau_m \ll 1$ but $\omega\tau_c$ is large. Thus our data with choice (2) c_∞ values are qualitatively consistent with cooperative glass dynamics like those observed in RADP.[13] A quantitative test of this model is given in Fig. 14 for the $x=0.60$ sample, where low T data are available at several frequencies.

V. SUMMARY AND CONCLUSION

Ultrasonic shear velocity and attenuation measurements have been made to characterize the dynamic cooperative behavior in $K_xNa_{1-x}CN$ mixed single crystals. In one sample ($x=0.88$), long-range orientational ordering occurs. In four other samples in the range $0.15<x<0.87$, an orientational glass phase is formed at low temperatures.

The $x=0.88$ sample exhibits critical slowing down of the quadrupolar relaxation with a dynamic exponent $z\nu=4.5$. This unconventional value, which differs significantly from the van Hove value $z\nu=1$ observed in bilinear coupled systems like KDP, is comparable to the $z\nu=3.7$ value for $Rb(CN)_{0.79}Br_{0.21}$ and may be related to the spin-glass value (predicted $z\nu=3$–4).

For glass-forming samples, the shear attenuation increases dramatically on cooling the paraelastic phase, goes through a maximum near T_g, and decreases very rapidly on further cooling in the glass phase. Associated with this attenuation behavior, the c_{44} shear stiffness exhibits a broad minimum and frequency-dependent dispersion near T_g. Unfortunately, the attenuation becomes so large that no ultrasonic data could be obtained over a range of ~55 K centered around T_g. Analysis of the data above this gap shows that the relaxation time τ_s in the high-temperature paraelastic phase varies rapidly with T according to the empirical form $\ln\tau_s = A_s - B_s T$ over a range of ~35 K. Analysis of data below the gap shows that the low-temperature glass phase data are consistent with very long relaxation times and a very broad distribution of relaxation times.

The dynamic behavior of this orientational quadrupolar glass is compatible with that observed for the dipolar glass RADP. Although there are not yet enough experimental data available to define uniquely the orientational glass phase dynamics, an attractive and plausible preliminary picture can be drawn.

ACKNOWLEDGMENTS

This work was supported by the National Science Foundation under Grant No. DMR-87-10035. The authors wish to thank J. F. Berret, K. Knorr, K. H. Michel, and R. Pick for helpful discussions.

[1]F. Lüty and J. Ortiz-Lopez, Phys. Rev. Lett. **50**, 1289 (1983).
[2]J. Ortiz-Lopez and F. Lüty, Phys. Rev. B **37**, 5461 (1988).
[3]A. Loidl, T. Schräder, R. Böhmer, K. Knorr, J. K. Kjems, and R. Born, Phys. Rev. B **34**, 1238 (1986).
[4]T. Schräder, A. Loidl, and T. Vogt, Phys. Rev. B **39**, 6186 (1989); T. Schräder, A. Loidl, T. Vogt, and V. Franck, Physica B **157**, 195 (1989).
[5]J. Hessinger and K. Knorr, Phys. Rev. Lett. **63**, 2749 (1989).
[6]J. Knorr, Physica Scripta T **19**, 531 (1987); A. Loidl, Annu. Rev. Phys. Chem. **40**, 29 (1989).
[7]J. F. Berret and R. Feile, Z. Phys. B **80**, 203 (1990).
[8]Z. Hu, C. W. Garland, and A. Wells, Phys. Rev. B **40**, 5757 (1989).
[9]C. W. Garland, J. O. Fossum, and A. Wells, Phys. Rev. B **38**, 5640 (1988).
[10]J. O. Fossum, A. Wells, and C. W. Garland, Phys. Rev. B **38**, 412 (1988).
[11]K. H. Michel, Phys. Rev. Lett. **57**, 2188 (1986); Phys. Rev. B **35**, 1405 (1987); **35**, 1414 (1987).
[12]K. H. Michel, Z. Phys. B **68**, 259 (1987); C. Bostoen and K. H. Michel, *ibid.* **71**, 369 (1988); K. H. Michel (private communication).
[13]E. Courtens and H. Vogt, Z. Phys. B **62**, 143 (1986); E. Courtens, R. Vacher, and Y. Dagorn, Phys. Rev. B **33**, 7625 (1986); E. Courtens and R. Vacher, *ibid.* **35**, 7271 (1987).
[14]C. W. Garland, J. O. Fossum, Z. Hu, and A. Wells, Phys. Rev. B **41**, 12 210 (1990).
[15]The quantity b, called β in Ref. 10, is given by $b \equiv \gamma^2/c^b = (T_c - T_0)/C$, where γ is the bilinear coupling constant, C is the Curie constant, and $(T_c - T_0)$ is the difference between coupled and uncoupled transition temperatures.
[16]E. Litov and C. W. Garland, Ferroelectrics **72**, 19 (1987).
[17]J. O. Fossum, J. Phys. C **18**, 5531 (1985); J. Hu, J. O. Fossum, C. W. Garland, and P. W. Wallace, Phys. Rev. B **33**, 6331 (1986); Z. Hu, C. W. Garland, and S. Hirotsu, *ibid.* **42**, 8350 (1990).
[18]P. C. Hohenberg and B. I. Halperin, Rev. Mod. Phys. **49**, 435 (1977); E. D. Siggia and D. R. Nelson, Phys. Rev. B **15**, 1427 (1977).
[19]A. Zippelius, Phys. Rev. B **29**, 2717 (1984); J. Souletie and J. L. Tholence, *ibid.* **32**, 516 (1985).
[20]K. Binder and A. P. Young, Rev. Mod. Phys. **58**, 801 (1986).
[21]J. K. Kruger, R. Jimenez, K. P. Bohn, J. Petersson, J. Albers, A. Klöpperpieper, E. Sauerland, and H. E. Müser, Phys. Rev. B **42**, 8537 (1990).
[22]C. W. Garland, J. Z. Kwiecien, and J. C. Damien, Phys. Rev. B **25**, 5818 (1982).
[23]T. Schräder, A. Loidl, and T. Vogt, Z. Phys. B **79**, 423 (1990).
[24]A. Cheng, M. L. Klein, and L. J. Lewis, Phys. Rev. Lett. **66**, 624 (1991).
[25]C. W. Garland, in *Physical Acoustics,* W. P. Mason and R. V. Thurston (Academic, New York 1970), Vol. 7, p. 51; B. Luthi and W. Rehwald, in *Structural Phase Transitions I,* edited by K. A. Müller and H. Thomas (Springer, Berlin, 1981).
[26]J. Hessingar and K. Knorr, Phys. Rev. Lett. **65**, 2674 (1990).